

# Accurate EM modelling of a not-fully accessible RF body coil at 3T for quantitative SAR investigations

Antonino Mario Cassara<sup>1</sup>, Gerd Weidemann<sup>1</sup>, Frank Seifert<sup>1</sup>, and Bernd Ittermann<sup>1</sup>

<sup>1</sup>Physikalisch-Technische Bundesanstalt (PTB), Berlin, Germany

**Target:** MRI scientists interested in the modeling of not accessible body coils of MRI clinical scanners for quantitative SAR predictions

**Purpose** Quantitative safety issues in MRI concerning SAR in complex contexts (e.g. presence of implants) can, at present, be only addressed using precise computational models of RF coils and their environment. Often, however, modelers have no direct access to many coil details (losses, lumped elements, feeding conditions, etc). This work describes different levels of modeling of the clinically most relevant Tx coil, the body coil, while feedback from quantitative RF measurements on only accessible ports was utilized to improve the accuracy. Results concerning  $B_1^+$  field distributions in a body phantom are compared to measured data.

**Methods** Numerical simulations of the body coil (BC) of 3T whole-body scanner (Magnetom Verio, Siemens, Erlangen) using the FIT scheme were performed using Microwave Studio (CST, Darmstadt, DE) and two coil models. The "generic" model included only details provided by the manufacturer i.e. a) the generic coil geometry; b) the value of the end ring capacitors; c) the position of the feeding ports and the phase relations between the two channels for two specific operational modes (circular or elliptic polarization) of the birdcage. This model was then modified to consider: d) the general loading conditions for the matching/tuning/decoupling (MTD) procedure and e) the position of the MTD trimmers. During our investigation we determined/refined: f) the precise value of the end ring capacitors using co-simulations (ADS, Agilent Technologies, Santa Clara, US); g) the value of the trimmer for the MTD procedure; and h) precise feeding conditions (relative phases and amplitudes) for the two modes, from voltage measurements with an oscilloscope. A last, important refinement was then achieved by including the coil losses (distributed resistors, lossy materials). The latter information was extracted from measured impedances at accessible cables toward the feeding ports and from S-parameters and Q-factors ratios using a network analyzer. Comparisons between the simulated internal  $B_1^+$  fields and measurements were performed on a ASTM-type body phantom filled with tissue-miming liquid (Tween20 solution,  $\epsilon=0.61$ ,  $\sigma=0.81$  S/m), placed at 5 different longitudinal positions. A specific  $B_1^+$  mapping technique and fitting routines were designed to accommodate the considerable off-resonance effects in large phantoms. In addition, the simulations were compared to point-wise  $E$  and  $B$  field measurements (all components, amplitudes and phases) outside of the phantom using time-domain field probes.

**Results** For one phantom position and elliptic polarization, Fig. 1 illustrates the averaged residuals (in %) between simulated and calculated  $B_1^+$  fields along the x (left-right) axis within an axial plane through the iso-center ( $z=0$ ) position. Averages and RMS (error bars) are calculated integrating the residuals (absolute values) profiles along the y-coordinate. With only the manufacturer's direct information, accuracy is limited, on the average, to about 30%-40% (Fig. 1, left graph, green curve). Adding information about measured (and slightly asymmetric) power attenuations between both channels and checking for optimal phase relations, reduced the deviations by almost a factor of 2 (Fig. 1, left graph, black curve). When including losses the accuracy ameliorates noticeably (Fig. 1, right graph, black curve). Remaining discrepancies of about 5% are probably due to known sources of error (positioning mainly) and could be further reduced. Figure 2 compares measured and simulated  $B_1^+$  maps in the transversal plane at  $z=0$  when either the "body" or the "head" section of the ASTM phantom were placed at that position, using the most accurate model. Some modeling problems were encountered when comparing simulated S and Z-parameters with measurements. Even if not needed, a procedure was created to verify the possible position of the feeding ports, in case this information would not have been available. Measurements with additional E- and H- field measurements are currently being prepared to test the model accuracy further, also outside the phantom.

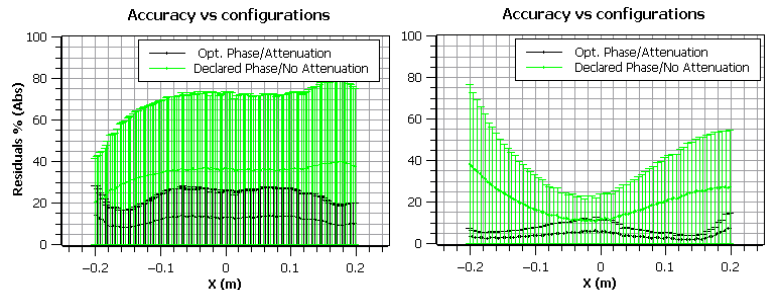


Figure 1: Left: generic coil model, no losses included; Right: "exact" coil model, losses included

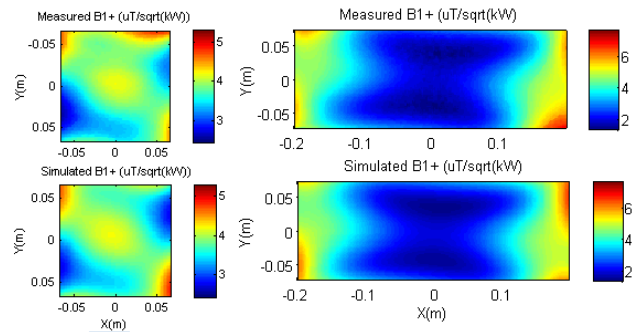


Figure 2. B1+ field distributions in head (left) and body (right) regions

**Conclusions** The coil model completed with additional information coming from measurements and optimization, largely improves predictive accuracy. Coil models reconstructed with this procedure can be used for quantitative comparisons of different SAR models in safety investigations for metrological purposes. An accuracy of <10% (almost) everywhere was achieved without any scaling or other free parameters even though many details of the manufacturer built coil were a priori not known. This work supports the idea that future directives or guidelines on MRI safety and SAR calculation should include a list of procedures (in-situ measurements) to quantify RF coil properties and the accuracy of the simulations, thus assisting modelers in creating accurate coil models for quantitative SAR analysis.

**Acknowledgments** The work was funded by the European Metrology Research Program (EMRP) grant HLT06. The EMRP is jointly funded by the EMRP participating countries within EURAMET and the European Union.